Accuracy of Robotic-Assisted Spinal Surgery––Comparison to TJR Robotics, da Vinci Robotics, and Optoelectronic Laboratory Robotics

Bryan W. Cunningham, Daina M. Brooks and Paul C. McAfee

Int J Spine Surg published online 4 October 2021
https://www.ijssurgery.com/content/early/2021/10/01/8139

The International Journal of Spine Surgery
2397 Waterbury Circle, Suite 1,
Aurora, IL 60504, Phone: +1-630-375-1432

International Journal of Spine Surgery, Vol. 00, No. 00, 0000, pp. 000–000
https://doi.org/10.14444/8139

Accuracy of Robotic-Assisted Spinal Surgery—Comparison to TJR Robotics, da Vinci Robotics, and Optoelectronic Laboratory Robotics

BRYAN W. CUNNINGHAM, PHD,[1,2] DAINA M. BROOKS, MEM,[1] PAUL C. MCAFEE, MD, MBA[1,2]

[1]*Musculoskeletal Education Center, Department of Orthopaedic Surgery, MedStar Union Memorial Hospital, Baltimore, Maryland,* [2]*Department of Orthopaedic Surgery, Georgetown University School of Medicine, Washington, D.C.*

ABSTRACT

Background: The optoelectronic camera source and data interpolation serve as the foundation for navigational integrity in the robotic-assisted surgical platform. The objective of the current systematic review serves to provide a basis for the numerical disparity that exists when comparing the intrinsic accuracy of optoelectronic cameras: accuracy observed in the laboratory setting versus accuracy in the clinical operative environment. It is postulated that there exists a greater number of connections in the optoelectronic kinematic chain when analyzing the clinical operative environment to the laboratory setting. This increase in data interpolation, coupled with intraoperative workflow challenges, reduces the degree of accuracy based on surgical application and to that observed in controlled musculoskeletal kinematic laboratory investigations.

Methods: Review of the PubMed and Cochrane Library research databases was performed. The exhaustive literature compilation obtained was then vetted to reduce redundancies and categorized into topics of intrinsic optoelectronic accuracy, registration accuracy, musculoskeletal kinematic platforms, and clinical operative platforms.

Results: A total of 147 references make up the basis for the current analysis. Regardless of application, the common denominators affecting overall optoelectronic accuracy are intrinsic accuracy, registration accuracy, and application accuracy. Intrinsic accuracy of optoelectronic tracking equaled or was less than 0.1 mm of translation and 0.1° of rotation per fiducial. Controlled laboratory platforms reported 0.1 to 0.5 mm of translation and 0.1°–1.0° of rotation per array. There is a huge falloff in clinical applications: accuracy in robotic-assisted spinal surgery reported 1.5 to 6.0 mm of translation and 1.5° to 5.0° of rotation when comparing planned to final implant position. Total Joint Robotics and da Vinci urologic robotics computed accuracy, as predicted, lies between these two extremes—1.02 mm for da Vinci and 2 mm for MAKO.

Conclusions: Navigational integrity and maintenance of fidelity of optoelectronic data is the cornerstone of robotic-assisted spinal surgery. Transitioning from controlled laboratory to clinical operative environments requires an increased number of steps in the optoelectronic kinematic chain and error potential. Diligence in planning, fiducial positioning, system registration, and intraoperative workflow have the potential to improve accuracy and decrease disparity between planned and final implant position. The key determining factors limiting navigation resolution accuracy are highlighted by this Cochrane research analysis.

Research Article

Keywords: optoelectronic accuracy, spinal surgery, imaging, navigation, robotics

INTRODUCTION

The fundamental technological challenge of navigation and robotic-assisted spinal surgery is that the virtual world needs to clearly represent the physical, real-time world. Among the multiple applications, variables, and equipment used in navigation and robotic-assisted spinal surgery, the optoelectronic camera source and data interpolation process serves as the foundation for navigational integrity and accuracy (or lack thereof) in the surgical platform. The spectrum of optoelectronic technology platforms is quite diverse, with use in sports performance activities such as speed skating and soccer,[1–4] human ergonomics,[5,6] clinical gait and motion analysis,[7–12] musculoskeletal kinematics,[13–20] and clinical operative procedures.[21–44] To this end, the degree of accuracy and errors acceptable across optoelectronic motion measurement platforms differ considerably based on application.[1] For example, fiducial arrays placed on anatomic pelvic landmarks of alpine skiers reported translation accuracy and errors of 8.37 ± 7.1 mm.[45] Although considered adequate for the evaluation of

positional or orientation-related differences in this athletic application, discrepancies of this magnitude would be unacceptable in the clinical operative setting. Technological advancements in the accuracy of optoelectronic marker–based systems over the past 20 years have facilitated the adoption and application of these platforms to the field of robotic-assisted spinal surgery.[12,46,47] An ensuing plethora of journal publications have documented the safety, efficacy, and technical accuracy of navigation and robotic systems,[21–24,30–32,35,48–55] operative surgical applications,[25,33,56,57] and challenges of process workflow, learning curve, and training.[28,30,31,50,51]

Review of these publications reveals what could be defined as a significant discrepancy when comparing optoelectronic accuracy in the laboratory setting versus the clinical operative environment. An approximate 10-fold decrease in technical accuracy of final implant position ($\leq$2 mm) in the clinical operative environment was observed compared with controlled musculoskeletal kinematic studies ($\leq$0.2 mm) despite the use of nearly identical optoelectronic camera systems. Hence, the objective of the current systematic review serves to provide a basis for the numerical disparity that exists when comparing the intrinsic accuracy of optoelectronic cameras, accuracy observed in the laboratory setting, and accuracy in the clinical operative procedures. It is postulated that there exists a greater number of linkages in the optoelectronic kinematic chain when analyzing the clinical environment in the laboratory setting. This increase in data interpolation, coupled with intraoperative workflow challenges, reduces the degree of accuracy compared with that observed in controlled musculoskeletal kinematic laboratory investigations.

METHODS

A comprehensive systematic review of the PubMed and Cochrane Library research databases was performed. The time interval was unrestricted, but the majority of publications making up the basis of this analysis were from 2000 to the present. A combination of key search terms was stratified into the following: optoelectronic measurement systems, technical accuracy, experimental error, robotic-assisted surgery, spinal kinematics, and navigation. The search was limited to papers in the English language, indexed in peer-reviewed journals accessible through online searches, and all publications included required a bona fide PubMed identification (pmid) or digital object identifier (doi) citation. The exhaustive literature compilation obtained was then pooled in an EndNote file, vetted to reduce redundancies and categorized into topics pertinent to optoelectronic measurement system accuracy with specific reference to intrinsic accuracy, registration accuracy, musculoskeletal kinematic platforms, and clinical operative platforms. The primary tier for inclusion focused on publications that reported quantitative units of measure (microns, millimeters, and degrees) for intrinsic camera accuracy and tolerances, accuracy obtained in a controlled laboratory setting, and accuracy in the clinical operative setting. In various fields—spinal surgery, urologic surgery, and total joint replacement surgery—navigation and robotic accuracy are measured and compared with the Optotrak 3020 and Optotrak Certus systems (Northern Digital Instruments, Waterloo, Ontario, Canada). Several localized positions in a radiographic phantom are compared with the data acquired with the gold standard Optotrak systems. For example, individual da Vinci trials were registered to the mean Optotrak data using a rigid point-based registration method.

An extensive number of peer-reviewed journal publications have documented the use, efficacy, safety, and technical accuracy achieved with robotic-assisted spinal surgery. The focus in reviewing these publications was to highlight the technical accuracy observations and determine a basis for discrepancy between planned versus actual final implant position based on postoperative computed tomography (CT) images. In case studies where quantitative measurements were not reported, the Gertzbein and Robbins score (GRS) was adopted to calculate pedicle screw implant position.[58] According to the GRS classification, screws centered within the pedicle are considered grade A, $<$2 mm from center is a grade B, a breach from 2 to 4 mm is grade C, a breach from 4 to 6 mm is grade D, and $>$6 mm is grade E. Grades of A and B ($<$2-mm pedicle breach) are considered clinically acceptable, and all other grades indicate malposition.

RESULTS

Three-Dimensional Cartesian Rigid Body Transformations

The reported optoelectronic measurements of accuracy, errors, and methods to quantify these in the laboratory setting or clinical operative environ-

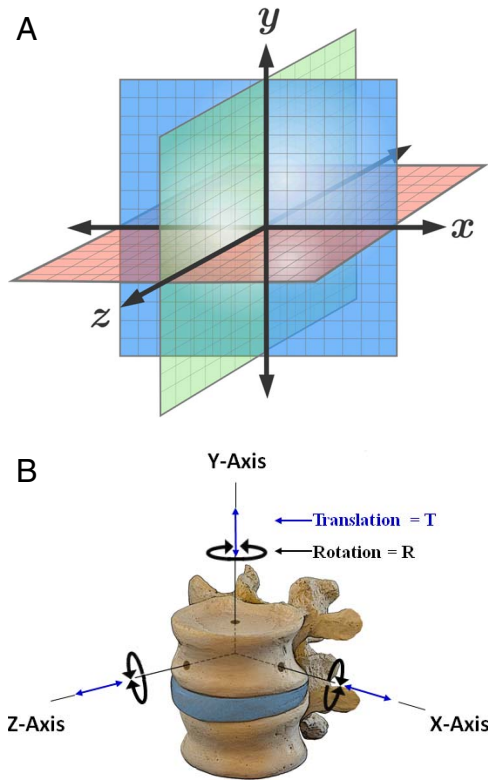

Figure 1. Cartesian Coordinate System and Conceptual Framework for Spinal Kinematics – Schematic representation of a fixed 3-dimensional Cartesian coordinate system for calculation of rigid body transformation in millimeters (mm) translation and degrees (deg) rotation along three orthogonal axes – X, Y and Z (A). This is in accordance to the axial (Y), sagittal (Z) and coronal (X) anatomic planes as defined by Panjabi's 3-dimensional conceptual framework for spinal kinematics (B).

ment are based on a fixed three-dimensional Cartesian coordinate system of rigid body transformation in millimeters of translation and degrees of rotation along three orthogonal axes: X, Y, and Z.[59–63] This is in accordance to the axial (Y), sagittal (Z), and coronal (X) anatomic planes as defined by Panjabi's three-dimensional conceptual framework for spinal kinematics (Figure 1).[64–66] From a nomenclature standpoint, accuracy is defined as a combination of trueness and precision according to the published International Organization for Standardization standard 5725-1.[67] Trueness refers to the difference between measured value and true position, typically represented by the mean value of repeated measurements. Precision is a measure of repeatability, typically represented by the standard deviation of repeated measurements, and refers to random error and noise within the system. In addition to these standardizations, a useful key measure with regard to accuracy (trueness and precision) is the root mean square distance error (RMS) as given by e_i being the three-dimensional distance error of measurement i and N the number of measurements:[68]

$$e_{\mathrm{RMS}} = \sqrt{\frac{1}{N}\sum_{1}^{N}(e_i \cdot e_i)}$$

Optoelectronic Measurement Systems

Image-guided surgery is based on the principle of integration and registration of the operative field to pre- or intraoperative data set (eg, CT or magnetic resonance imaging) via amalgamation of an optoelectronic imaging system with robotic platform.[69] Although not necessarily involved in the execution of operative procedures, optoelectronic measurement systems are considered the gold standard in motion capture accuracy[1,70] and provide three-dimensional visualization and guidance, improving task execution and targeting accuracy while functioning in a semiautonomous fashion.[71] Hence, objective accuracy and error assessments of optoelectronic-robotic interventional platforms is essential. The Optotrak 3020 with a 24 infrared light-emitting diode (IRED) pen probe has a National Institute of Standards and Technology traceable accuracy of 0.1 mm for a single IRED over the work volume and a 0.25-mm accuracy when localizing a 24-IRED helical pen probe. Regardless of optoelectronic camera system, the fundamental triad of common denominators in assessing platform accuracy include (1) intrinsic accuracy of the source device, (2) registration and tracking accuracy, and (3) application accuracy. Prior to addressing the basis for application accuracy across laboratory versus clinical platforms, the intrinsic and registration accuracy and potential for error propagation are of primary consideration.

Intrinsic (Technical) Accuracy

The initial link in the optoelectronic kinematic chain of data transference resides in the intrinsic accuracy of the camera source. Of the multiple factors affecting downstream optoelectronic accuracy in musculoskeletal kinematic and clinical operative platforms, the intrinsic camera components are most controllable. Mechanical compliance of the system, loose interconnection mechanisms,[69] variation in camera resolution, calibration, imperfect lenses, number of cameras, spatial orientation, noise, computer vision algorithms, and jitter all

represent sources of intrinsic error in optoelectronic systems.[47,69,72,73] Maletsky et al[74] reported the relative accuracy position between two rigid bodies at 0.03 mm of translation and 0.04° of angulation, respectively. As a baseline statement of comparison, the optoelectronic systems used in clinical operative or controlled laboratory platforms report only marginal differences in accuracy. Further, the contribution of intrinsic errors is of miniscule value in comparison to error(s) propagation secondary to registration: targeting tracking and application in controlled experimental and clinical operative platforms.

Registration Accuracy and Target Tracking

A second key step in the optoelectronic kinematic chain and highest probable link(s) of error propagation is the registration process. This intraoperative process integrates correlation and mapping algorithms to register the physical patient to the virtual patient via the navigation system, optoelectronic source, fiducial arrays in the operative field, and coregistration of the patient intraoperative X-rays with the preoperative CT images. Accurate, close-to-ideal reference reproducibility and fidelity of the data set improves trueness and precision of subsequent intraoperative tracking. Multiple factors affect registration accuracy and target tracking, including optoelectronic camera source, passive versus active arrays, occlusions, distance between fiducial arrays and camera source, static versus dynamic array localization, and anatomic locations of the coordinate reference fiducials.[1,35,44,55,68–81] For example, increasing the camera distance from 6 to 8 ft nearly triples the intrinsic registration error along the Z axis (maximum = 0.250 mm) for the Polaris passive fiducial array system. Hence, closer approximation of the optoelectronic camera source to the operative fiducial arrays ($\leq$6 ft, or approximately 1800 mm) minimizes jitter and improves precision.[82] In summary, propagation of computational measurement errors in the optoelectronic kinematic chain has a compounding effect for the following transitions: (1) measurement of the intrinsic image plane error secondary to errors within the optoelectronic system, (2) transitioning from image error to fiducial location error, and (3) transition from fiducial location error to tracking target error. The mathematical expressions for these computational transformations are beyond the scope of the current publication but are well documented by Fitzpatrick et al[77,79] and Sielhorst et al.[72] The margins of error secondary to intrinsic and registration accuracy in optoelectronics are more manageable compared with unpredictable factors related to application in the laboratory versus dynamic clinical intraoperative environments.

Application Accuracy: Basic Scientific Laboratory Platform

A plethora of publications have documented the biomechanical properties of the occipitocervical through lumbopelvic spine under controlled laboratory conditions using Panjabi's 3-dimensional conceptual framework for testing.[17,64–66,83] In contrast to the challenges of the clinical operative environment, motion analysis of spinal implant and anatomic vertebral structures(s) in the controlled laboratory setting is performed using a 6-degree-of-freedom musculoskeletal simulator interfaced with an optoelectronic measurement system. The fundamental principles pertinent to maximizing optoelectronic accuracy include mounting the specimen to a rigid testing platform, affixing active or passive fiducial arrays directly to implants or anatomic structures using screw-bolt fixation, and creating rigid body configurations parallel to the camera source. To this end, a series of laboratory investigations using the NDI Certus and Vicon MX13 camera systems (Vicon Motion Systems Ltd, Oxford, UK) reported the peak limits of optoelectronic accuracy when evaluating kinematics of the osteoligamentous spine.[13–19,84–90] Cunningham et al[14] compared occipital plate versus intracranial anchors for reconstruction of the occipitocervical (O-C) junction. The reported differences (degrees) in axial rotation at the O-C junction based on optoelectronic measurements were 4.13 $\pm$ 2.05 (intact), 0.22 $\pm$ 0.13 (plate), and 0.30 $\pm$ 0.21 (anchor). Rotation of the plate and anchor with respect to the occiput in flexion-extension ranged from 0.06 $\pm$ 0.05 to 0.10 $\pm$ 0.08, respectively. Although not of clinical significance, the study quantified differences on the order of 0.1° between 2 methods of occipitocervical fixation.

In a complex kinematic study using a Vicon optoelectronic system, La Barbera et al[18,19] investigated lumbar interbody cages with Ponte osteotomy versus pedicle subtraction osteotomy for severe sagittal imbalance. The peak accuracy of neutral zone measurements (degrees) across the intact L3–

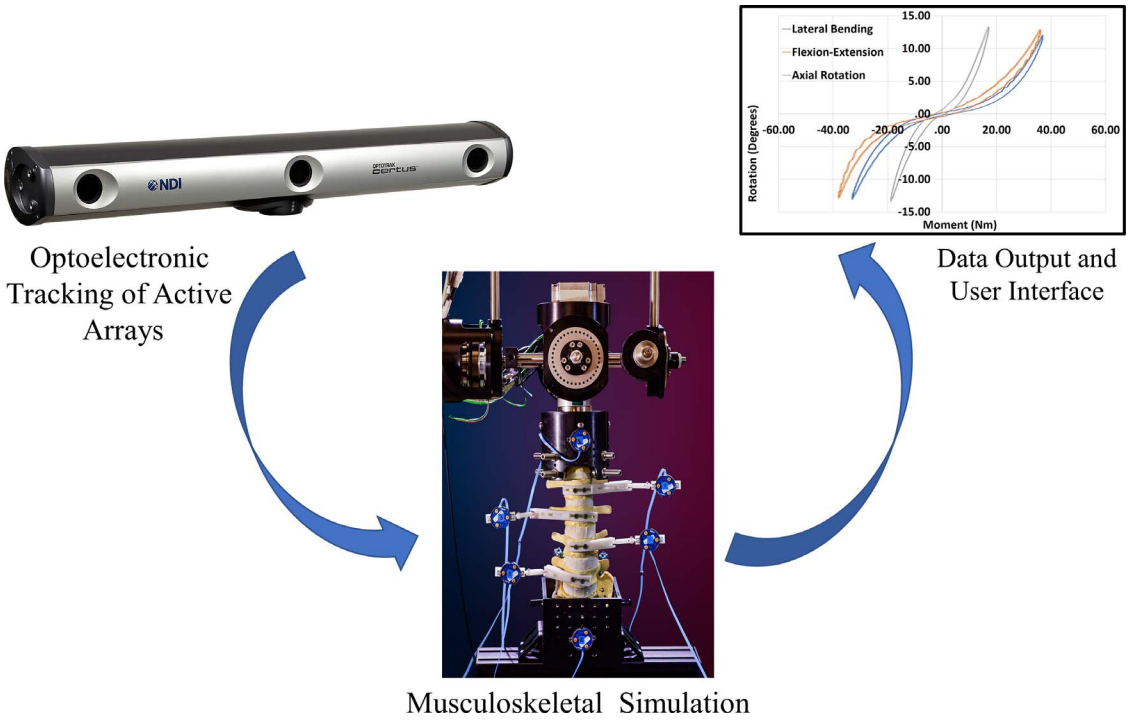

Figure 2. Laboratory Platform for Optoelectronic Data Transference Process - Schematic illustration demonstrating the laboratory workflow and process for data transference utilizing optoelectronic tracking. The camera source visualizes the active fiducial arrays affixed to the vertebral elements and transfers the data directly to the user interface for computational analysis. The collective effect of testing methodology and limited experimental coordinate transformations between data input / output reduces error propagation and maximizes optoelectronic accuracy.

L5 segments demonstrated values of 0.7 (range 0.3–1.9) in flexion-extension, 1.0 (range 0.1–3.8) in lateral bending, and 0.2 (range 0.1–0.9) in axial rotation in flexion-extension. Factors of specimen stabilization, alignment, camera resolution, proximity to fiducials, planar visualization of the active arrays, and controlled motion application account for the high degree of accuracy reported in these studies. Laboratory workflow methods and conditions for experimental musculoskeletal kinematic studies are streamlined and optimized for maximizing optoelectronic accuracy. Factors of specimen stabilization, alignment, camera resolution, proximity to fiducials, planar visualization of the active arrays, and controlled motion application account for the high degree of accuracy reported in these studies. The collective effect of testing methodology and limited experimental coordinate transformations between data input/output reduces error propagation and maximizes optoelectronic accuracy (Figure 2, Table).[91–97]

Application Accuracy: Clinical Operative Platform

Transitioning from controlled laboratory conditions to the dynamic variability of a clinical operative environment presents a different set of application challenges for maintaining peak optoelectronic accuracy. Unique to robotic-assisted surgery and in contrast to the laboratory setting, the intraoperative process requires considerably more steps in the transference of optoelectronic kinematic data. This complex process flow integrates correlation and mapping algorithms to register the physical patient to the virtual patient via the navigation system, optoelectronic source, surveillance markers, patient reference markers, end effector instruments in the operative field, and patient CT images. Accurate, close-to-ideal reference reproducibility and maintenance of this data set is the primary intraoperative objective and challenge. Despite the use of nearly identical optoelectronic sources and fiducial arrays, a consistent disparity exists when comparing the reported technical accuracies in the laboratory setting versus clinical operative environment. An approximate 10-fold decrease in accuracy was observed when comparing the final implant position ($\leq$2 mm) in the clinical operative environment with musculoskeletal kinematic studies ($\leq$0.2 mm). An extensive number of peer-reviewed journal publications have documented the use, efficacy, safety, and technical accuracy achieved with robotic-assisted sur-

Table. Robotic and navigation accuracy.

Application	Author/Year	Article Type	Measurement System	Numbers: Navigation Accuracy and Outcomes
Clinical operative setting				
Spinal surgery	Helm et al 2015[34]	Literature review	Optoelectronic measurement system	12 622 pedicle screws total: as planned: 93% <2 mm of plan: 3.1% >2–4 mm of plan: 0.72% 4–6 mm of plan: 0.43%
	Zhang et al 2020[35]	Systemic review of Prospective, retrospective, and randomized control trials	Optoelectronic measurement system	5013 pedicle screws total: as planned: 95.3% >2–6 mm of plan: 4.6%
	Devito et al 2010[36]	Prospective clinical study	Optoelectronic measurement system	646 pedicle screws total: as planned: 89.3% <2 mm of plan: 8.9% >2–4 mm of plan: 1.3% > 4 mm of plan: 0.31%
	Keric et al 2017[37]	Prospective clinical study	Optoelectronic measurement system	1857 pedicle screws total: <3 mm of plan: 96.9 >3–6 mm of plan: 2.0% > 6 mm of plan: 1.1%
	Tarawneh et al 2021[38]	Systematic review	Optoelectronic measurement system	Grade (A + B): robot-assisted group: 97% freehand technique: 95.4% ($P = .008$)
Total hip arthroplasty	Cozzi Lepri et al 2020[39]	Prospective clinical study	Optoelectronic measurement system	Intraoperative mean registration error: 0.2–0.6 mm Absolute discrepancy between robotic and radiographic assessments: leg length discrepancy: 1.3 ± 1.5 mm combined offset: 1.1 ± 0.9 mm
	Xu et al 2020[40]	Prospective clinical study	Optoelectronic measurement system	Target inclination: 40°; mean inclination achieved: 40.7° (±0.9°) Target inclination: 45°; mean inclination achieved: 45.3° (±1.0°)
Total knee arthroplasty	Deckey et al 2021[41]	Prospective clinical study	Optoelectronic measurement system	Robotic-assisted total knee arthroplasty versus standard total knee arthroplasty, respectively: mean femoral positioning: 0.9° (±1.2°) versus 1.7° (±1.1°) mean tibial positioning: 0.3° (±0.9°) versus 1.3° (±1.0°) mean posterior tibial slope:0.3° (±1.3°) versus 1.7° (±1.1°) mean mechanical axis limb alignment: 1.0° (±1.7°) versus 2.7° (±1.9°) (all $P < .001$)
	Jeon et al 2019[42]	Retrospective clinical study	Optoelectronic measurement system	Outlier prevalence for hip-knee-ankle angle: robot-assisted group: 10.7% conventional group: 16.5%
Neurosurgery	Goia et al 2018[43]	Retrospective clinical study	Optoelectronic measurement system	Distance between intended and actual location: right side: 0.81 mm left side: 1.12 mm
	Grunert et al 2003[44]	Clinical literature review	Optoelectronic measurement system	Intrinsic technical accuracy: 0.1–0.6 mm Registration accuracy: 0.2–3 mm Application accuracy: 0.6–10 mm
In vitro laboratory setting, basic scientific studies				
	La Barbera et al 2020[18,19]	In vitro lumbar cadaveric model	Optoelectronic measurement system	Flexion-extension: 0.7° (range 0.3°–1.9°) Lateral bending: 1.0° (range 0.1°–3.8°) Axial rotation: 0.2° (range 0.1°–0.9°)
	Lieberman et al 2006[30]	In vitro lumbar cadaveric model	Optoelectronic measurement system	Four screws deviated from surgeon's plan: 1.02 ± 0.56 mm (range 0–1.5 mm)
	Cunningham et al 2020[14]	In vitro cervical cadaveric model	Optoelectronic measurement system	Differences between two methods of occipitocervical fixation: 0.06 (±0.05°)

Table. Continued.

Application	> Author/Year	Article Type	Measurement System	Numbers: Navigation Accuracy and Outcomes
	Sun et al 2020[91]	Plastics and reconstruction, craniofacial surgery, 3-dimensional printed model and canine model	Robot-assisted 3-dimensional reconstructive frame	Outside position error: 1.71 ±0.16 mm Inside position error: 1.37 ±0.28 mm Orientation error: 3.04 ±1.02°
	Guo et al 2020[92]	Sports medicine, human cadaveric knee model	Optoelectronic measurement system	Robotic positioning accuracy in placing bone tunnels for ACL reconstruction: dry bone tunnels: 1.73 mm wet cadavers: 2.17 mm freehand anterior cruciate ligament reconnection: 6.46 mm
	Hampp et al 2019[93]	Total knee arthroplasty, human cadaveric knee model	Optoelectronic measurement system	Accuracy and precision to plan of robotic cohort versus manual cohort, respectively: Femoral components: coronal plane: 0.6° versus 2.6° sagittal plane: 1.1° versus 3.7° axial plane: 0.7° versus 3.4° Tibial components: coronal plane: 0.8° versus 1.0° sagittal plane: 1.4° versus 1.6°
	Miller et al 2016[94]	Cardiothoracic, swine model	Optoelectronic measurement system	Precise stent placement in all 8 animals
	Liu et al 2015[95]	Otolaryngology and transoral robotic, porcine model	Augmented reality	Resection ratios of mock tumor margins: image-guided robotic system: 1.00 control scenarios: 0.0 alternative methods of image guidance: 0.58
	Kalia et al 2020[96]	Urologic surgery, gelatin phantom	Augmented reality	Target registration error (TRE): 4.56 ± 1.57 mm TRE x-direction: 1.93 ±1.26 mm TRE y-direction: 2.04 ±1.37 mm TRE z-direction: 2.94 ±1.84 mm
	Kwartowitz et al 2006[98]	Phantom (da Vinci Classic)	Robotic telesurgery	Mean localization error (da Vinci Classic): internal comparison: 1.02 mm fiducial registration error: 1.31 mm target registration error: 1.35 mm
	Kwartowitz et al 2007[99]	Phantom (da Vinci S)	Robotic telesurgery	Mean localization error (da Vinci S): internal comparison: 1.05 mm fiducial registration error: 1.31 mm target registration error: 1.25 mm
	Diakov et al 2019[97]	Neurosurgery, skull phantom	Optoelectronic measurement system	Registration error for entire head: 1.5 mm

gery.[23,28,30,34–44,48,50–52,55,56,100–127] The focus in reviewing these publications across multiple robotic-assisted surgical platforms is to highlight the technical accuracy and discrepancy between planned versus actual final implant position (Table).

Based on the GRS system for transpedicular screw accuracy, Helm et al[34] performed a comprehensive literature review on the technical accuracy of 1 622 pedicle screws implanted using a variety of image-guided surgery navigation systems. As reported, 11 830 were positioned Ideal according to preoperative plan (A), 395 screws within less than 2 mm of plan (B), 92 breached between 2 and 4 mm off center (C), and 55 were within 4 to 6 mm of the preoperative plan (Table). Grades of Ideal and A (<2mm of plan) indicated "no perforations" and were considered acceptable in these anatomical segments according to Helm and coworkers. As a study limitation to the Helm et al publication, the paradigm of 3-dimensional accuracy as reported by Jiang et al[128] is a more suitable and accurate description for pedicle screw placement versus accuracy based on single-plane imaging.

The time-honored tenet of pedicle screw deformity surgery, compared with European techniques for decades, was "probe rather than drill" the pedicle. This proved to be easier to learn and safer, as the surgeon could use a blunt probe and stay within the intramedullary canal of the pedicle and "increase accuracy." The accuracy and safety of

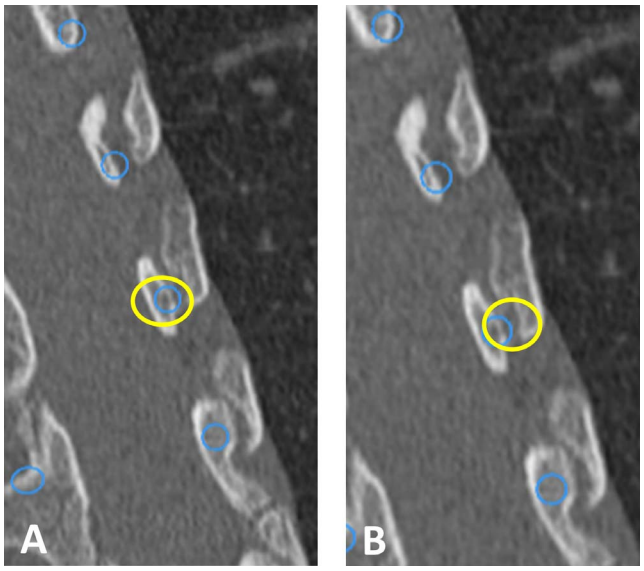

Figure 3. Computed Tomographic Images – Computed tomographic images demonstrating comparative pedicle screw insertion techniques of "Old School" versus "New School" methods. The Old School technique includes probing the center of the pedicle, intramedullary blunt pedicle finder, and concentrically expanding the pedicle to permit screw insertion (A). The New School navigated technique utilizes a more outside-in converging trajectory permitting preservation of the medial pedicle wall (B). Note the change in position of the circle defining region of insertion corridor.

pedicle screw insertion was defined as reducing the number of pedicle screw breaches.[129] With the advent of navigation and robotics, this definition has to be adapted to more contemporary goals (Figure 3). It is now possible to safely insert 4.5-mm-diameter pedicle screws into 3.0-mm thoracic pedicles by using navigated outside-in techniques, incorporating the entire costovertebral joint complex as a navigated target. Using a more tangential, outside-in converging trajectory, longer screws can be implanted compared with the previous "old-school," nonnavigated techniques. Probing the pedicle and starting in the middle of the pedicle intramedullary canal allows the surgeon to concentrically enlarge the hole starting in the center. Unfortunately, using this old-school technique, the spinal canal can be breached in adolescent idiopathic scoliotic deformities, particularly on the convex side from T1 to T6, where the pedicles tend to be hypoplastic. With navigation, surgeons can optimize screw size in the upper thoracic pedicles: "drill to preserve the medial pedicle wall." The precise, pinpoint location where the robot starts with orientation to the transverse process and superior articular process is unique to each pedicle. It is not in the center of the pedicle unless transpedicular depth and diameter are of sufficient dimension. The pedicle starting point, size, and optimal trajectory are planned based on a 3-dimensional virtual spine digitally constructed from a preoperative or early intraoperative CT scan. The starting point is unique to each pedicle screw and more tangential, especially in the cervical spine, compared with freehand techniques. The navigated trajectory is directed medial into the vertebral body and often more cranial—difficult to predict and accomplish freehand—which allows for improved purchase without violation of the medial wall. Using navigation and robotics in deformity procedures, the "new navigated school" allows for precise placement of costovertebral screws into the vertebral body. Therefore, the accuracy of robotic pedicle screw placement is based on the planned versus actual screw implant location, avoidance of a medial pedicle wall breach, and obtaining optimal fixation. The Gertzbein and Robbins quantitative scale of pedicle screw accuracy is not appropriate in the navigated school of robotic surgery, where intentional breach of the lateral pedicle and navigation of the pedicle screw into the costotransverse joint complex is intentional (Figure 4). This quantitative scale would result in a 100% intentional lateral breach despite increased fixation and correction of the scoliotic curve.

In robotic-assisted total hip arthroplasty, Cozzi Lepri et al[39] calculated differences between planned and actual measurements in leg length of 1.3 ± 1.5-mm displacement and target inclination of 0.3° to 0.7° angulation. As reported by Goia et al,[43] for neurosurgical applications in deep brain stimulation, the difference between planned and actual lead implantations positions was on the order of 0.8 to 1.12 mm of displacement (Table). For urologic surgical procedures, the da Vinci robot has the most extensive track record, with several generations of improvements.[130–132] As of December 2008, there were over 1000 da Vinci units sold, with well over 300 000 procedures performed. The most successful application of the robot is prostatectomy, with approximately 70% of all radical prostate removal procedures performed with the da Vinci in 2008 in the United States.[132] A typical comparison of accuracy between the new da Vinci S model (1.25 mm) and the da Vinci Classic model (1.35 mm) are shown in the Table.[98,99] As predicted, the intrinsic computed accuracy of the da Vinci urologic robot system is higher than robotic-assisted spinal applications (1.02 mm) but still not to the level of Optotrak (0.25 mm).[98] Da Vinci systems are in their

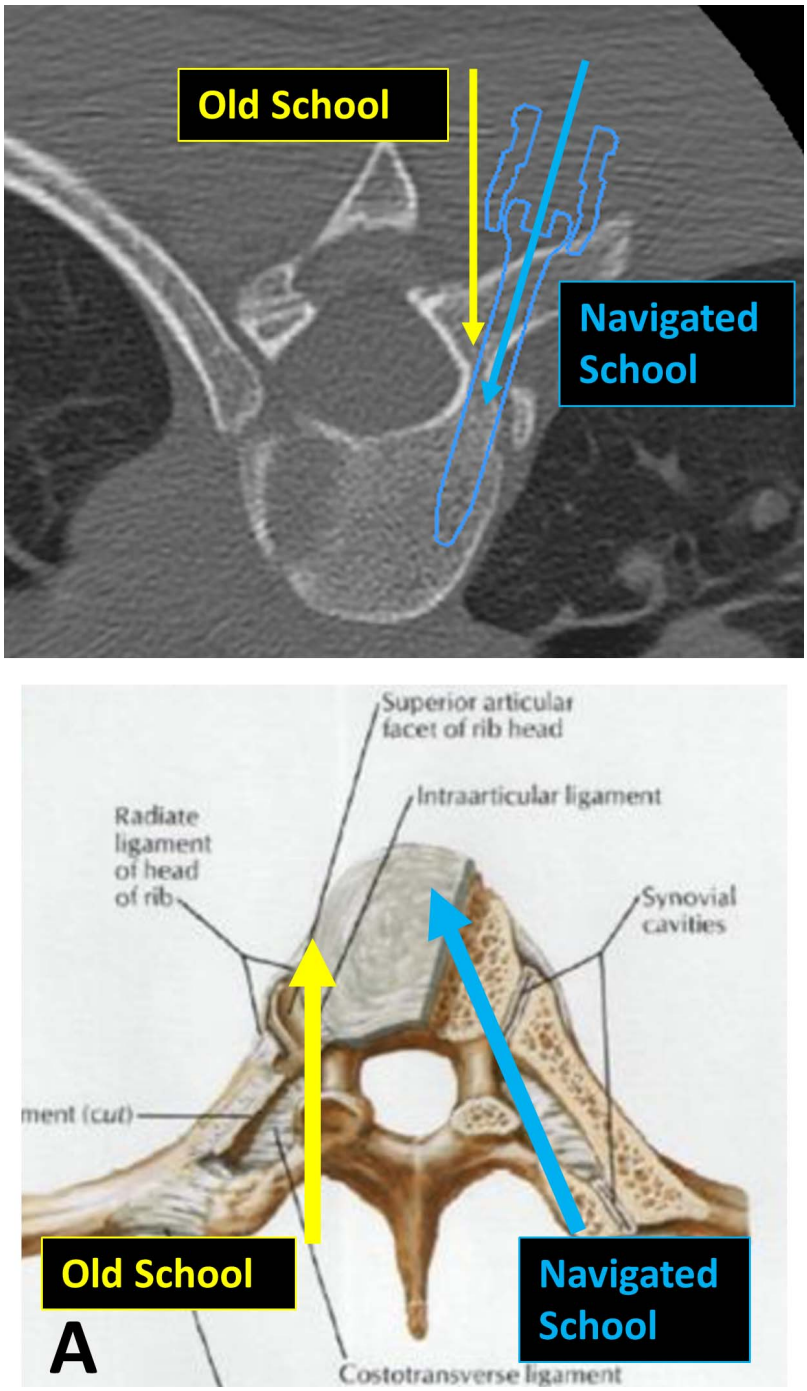

Figure 4. Computed Tomographic and Schematic Images of Pedicle Screw Trajectory – The New Navigated School permits the surgeon to maximize pedicular fixation by incorporation of the entire costovertebral complex as showing the computed axial tomographic and schematic illustrations (A). As such, longer and larger diameter pedicle screws (5.5mm versus 4.5mm) can be inserted, while avoiding breach of the medial pedicle wall (B).

third generation—it is anticipated that the accuracy of spinal navigation and robotics will demonstrate similar improvements over the same time period with iterative improvements. Importantly, the da Vinci is a master-slave robot that does not incorporate real-time optoelectronic camera tracking. The current systematic review compares the da Vinci with studies that have been done with optoelectronic camera systems; however, this paradigm is not directly comparable to a real-time image-guided system that is used in spinal surgery. A direct comparison of accuracy between these 2 different robotic systems is challenging, as 2 different things are being compared (movement of

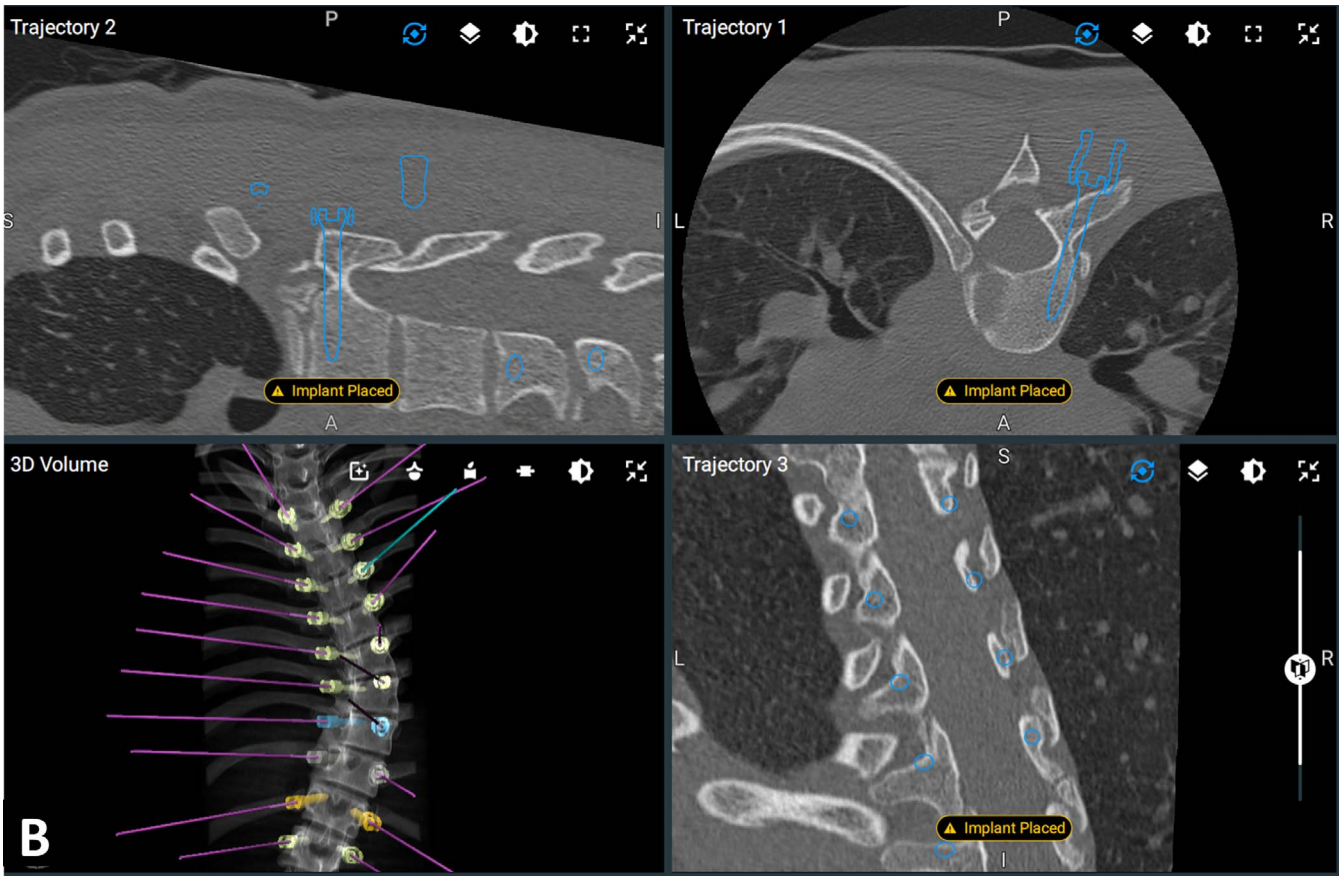

Figure 4. Continued.

a robotic arm in the case of the da Vinci and accuracy of screw placement in the case of a spine robot). While "accuracy" inferences can be made, a direct comparison between different robotic systems in different surgical subspecialties needs to take into account different definitions of "accuracy."

The continuation in the adoption of navigation and robotic-assisted surgical procedures is ensured, as there is space for improvement in the accuracy based on Cunningham and Brooks's[133] meta-analysis, which establishes the basic scientific accuracy: 0.1 mm of translation and 0.1° degree of rotation in optoelectronic laboratory conditions. Despite the use of nearly identical optoelectronic systems in the laboratory and clinical settings, the precision falls off in clinical spine applications to 3 to 4 mm translation and 2° to 3° of rotational accuracy. Robotic-assisted total joint replacement currently lies between these 2 extremes. Total joint robotics does not involve viscoelastic joints (3-joint complexes similar to the functional spinal unit) and does not involve a series of chain linkages between the navigated bone and skeletally anchored reference fiducials. Hence, the basis for the disparity and continuum of accuracy when transitioning from the controlled laboratory setting to the clinical operative environment is secondary to an increased number of steps in the optoelectronic kinematic chain and potential for error propagation in experimental coordinate transformations. Moreover, intraoperative challenges of array location, system registration, spinal flexibility, anatomic topography, and workflow affect navigational integrity and provide a basis for the disparity of optoelectronic accuracy in the clinical environment compared with the controlled laboratory setting. Collectively, these factors result in a continuum of optoelectronic accuracy with the greatest degree of accuracy observed in the laboratory setting and the least in the clinical operative spine environment (Table).

Basis for Disparity in Optoelectronic Accuracy

A key consideration pertaining to optoelectronic accuracy in the clinical environment compared with the laboratory setting is the dynamic nature of the operating room. The basis for disparity in accuracy

when equating the laboratory versus clinical operative platforms is a result of the combined, cumulative errors secondary to the intraoperative workflow process, variability in anatomic morphology, and spinal flexibility. Of fundamental importance and the crux of the matter related to error propagation in navigation and robotic-assisted spinal surgery is the assumption that the workflow platform and patient's spine are rigid, and, as such, motion of any type is perceived as a rigid body transformation. Optoelectronic error reduction in the clinical flow requires stabilization of the camera source, rigid fixation of surveillance arrays in the iliac crest, stable attachment of patient reference and registration arrays to anatomic landmarks, and end effector instruments arrays that are inflexible. The end effector is the last link where the robotic enters the work space, and small rotations or translations in the array references can lead to large errors in instrument position. Although accurate, close-to-ideal reference reproducibility of these steps will reduce errors, the reality is that fixed arrays do move, leading to increased relative motions between arrays and subsequent error propagation and disparity between the physical, real-time world and the virtual world. Moreover, spatial errors can be further magnified due to geometrical distortion of preoperative images and tracking error of the surgical instruments.[134] To register the physical patient to the virtual patient, Grunert et al[44] proposed a series of transformation matrices, including fiducial-based paired-point transformation, surface contour matching, and hybrid transformation. The hybrid transformation process is most applicable to robotic-assisted spinal surgery, as it includes the methods of surface-based and pair-point–based methods with implanted fiducials. As such, tracing at least 3 anatomic landmarks with navigational confirmation serves to reduce error potential.

Several publications on optimizing clinical workflow process have been reported.[31,49,53,134–138] Lieberman et al[31] provides an excellent description of the step-by-step workflow process in robotic-assisted spinal surgery. The report provides a concise methodological approach to operative workflow while at the same time providing a collective basis for potential error(s) propagation in the clinical setting. The sequential description of process flow/error potentials includes preoperative and intraoperative registration, dislodgement of reference arrays, damaged or bent navigation tools[139–141] and array occlusions (eg, distance and blood), skiving or tool deflection secondary to sloped anatomic topology or muscle retraction, and untracked patient movement during the spinal destabilizing procedure. In addition to unintended motion or bending of fiducial arrays, the inherent differences in anatomic topology, bone mineral density, and flexibility of the patient's spine, both before and following destabilization and reconstruction procedures, cannot be overemphasized. The challenge is that the spine is often flexible—the drill and robotic arm may be properly located, but highly mobile, multisegmental spinal reconstructions with minimal deflection force lead to unintended rotation or translation of the operative vertebral elements, skiving, or tool deflection and affects precision rate during screw insertion.[31,49,136,137,140,142,143] The basis for decreased technical accuracy in the clinical operative platforms is a result of combined, cumulative errors secondary to the intraoperative workflow process, the number of kinematic linkages, and variability in patient spinal morphology and flexibility (Figure 5).

DISCUSSION

In reviewing the intrinsic technical accuracy and registration accuracy, there exists a substantial burden of proof that the potential performance in optoelectronics is nearly identical between the two platforms—laboratory versus clinical operative—under static conditions. The downstream difference in optoelectronic technical accuracy and disparity between the 2 platforms is secondary to the dynamic factors unique to each. The laboratory workflow methods and array registration for experimental basic scientific studies are rigid and highly controlled with limited experimental coordinate transformations between data input/output, reducing error propagation and maximizing optoelectronic accuracy. Unique to robotic-assisted spinal surgery, the dynamic intraoperative process necessitates considerably more steps in the transference of optoelectronic kinematic data. The complex data flow process integrates correlation and mapping algorithms to register the physical patient to the virtual patient via the navigation system, optoelectronic source, surveillance markers, patient reference markers, end effector instruments, and patient CT images. Essentially, this is a comparison of technical accuracy between a rigid, highly controlled

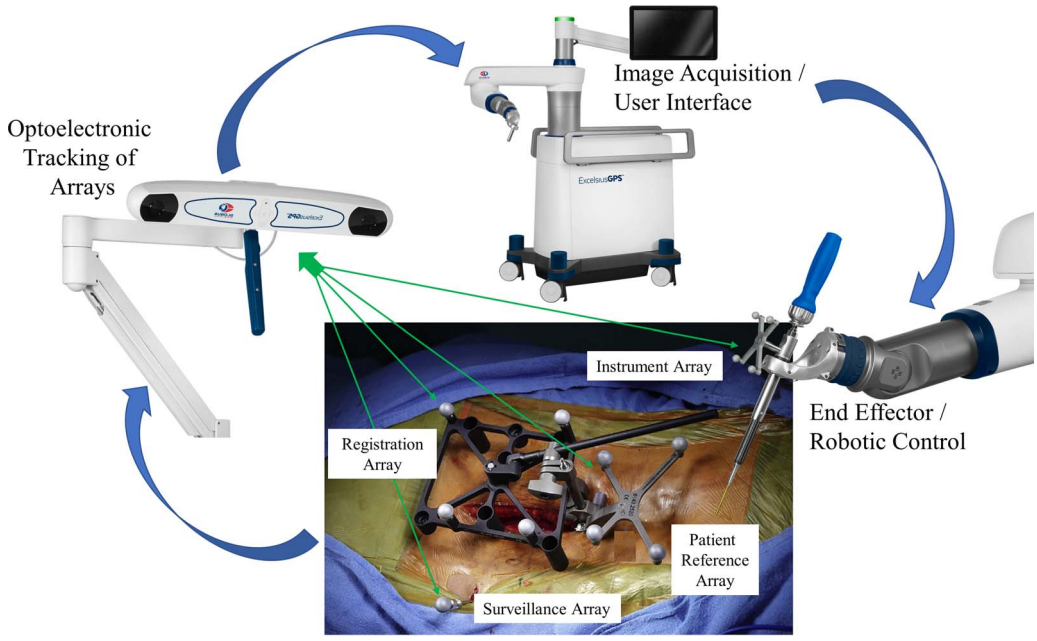

Figure 5. Clinical Platform for Optoelectronic Data Transference Process – Schematic illustration demonstrating the operative clinical workflow and process for data transference utilizing optoelectronic tracking. Unique to robotic-assisted surgery and in difference to the laboratory setting, the intra-operative process requires considerably more steps in the transference of optoelectronic kinematic data. This complex workflow process integrates correlation and mapping algorithms to register the physical patient to the virtual patient via the navigation system, optoelectronic source, surveillance markers, patient reference markers, end effector instruments in the operative field, and patient CT images. Accurate, close-to-ideal reference reproducibility and maintenance of this dataset is the primary intra-operative objective and challenge.

setting and a variable environment with multiple data input factors. The collective effect results in an increased potential for error propagation from experimental coordinate transformations, data processing, and optoelectronic kinematic linkages in the clinical setting.

There is significant potential for clinical improvements in spinal navigation and robotics. The current challenges as addressed in this Special Focus Issue are multifactorial:

1. The patient's thoracic spine moves under anesthesia with respirations as the chest cavity expands. This decreases the accuracy of placing pedicle screws on the upper convex side of adolescents with scoliotic curves.
2. An increased number of skeletally based reference fiducials are necessary and located closer to the target site.
3. Intervening spinal motion above and below spinal anchors, that is, Mazor L3–L4 motion when the Hover-T frame spans from the 2 pelvic Steinmann pins (PSIS) to the T12 spinous process (K-wire). The intercalated spinal segments that are bridged are free to move.
4. Need additional confirmatory skeletal reference fiducials to prevent skiving.
5. Learning through artificial intelligence would permit progressive incorporation of information as each pedicle screw is successfully inserted. The successive introduction of each pedicle screw should be merged into virtual information – leading to increased accuracy.
6. Clinical accuracy of robotics and navigation is not solely related to robotic sophistication. Fluoroscopic resolution used in registration and merging of the virtual data intraoperatively is often the gating item. Improvement in intraoperative 3-dimensional CT would increase accuracy and decrease operative time.

The future of spine robotics and navigation is essentially here—one only has to look at other fields. For example, otolaryngology has used electromagnetic fields for navigation rather than infrared camera capture of reflective skeletal fiducials. For intraoral resection of tumors, electromagnetic fields are advantageous, as they allow the advantage of non–line-of-sight navigation. This allows the surgeon to navigate around a corner or, in the case of otolaryngology, down the hypopharynx. There are 2 disadvantages of electromagnetic field navigation that have to be solved before this

non–line-of-sight technology can be used in spine surgery. First, there cannot be ferromagnetic instruments in the field. Second, the distance (≤12 in) between the end effector and the field generator has to be reduced in order to have accurate navigation. The line-of-sight requirement for spinal navigation is a significant obstacle in current technology; it is invigorating that other surgical specialties are able to work through this obstacle.

There are several recent prospective randomized multi-institutional MIS trials that have relevance in the area of safety and accuracy of navigation and robotics. Good et al[144] in their MIS ReFRESH study compared the complications and revision rates from Mazor robotics in 485 patients—374 robotic guidance arm and 111 patients in a fluoroscopy guidance arm from 9 sites. Fluoroscopic time per screw during instrumentation was 3.6 ± 3.9 s with Mazor compared with 17.8 ± 9 s with fluoro-guidance, indicating an 80% reduction in intraoperative radiation per screw ($P < .001$). During the first postoperative year, robotic guidance led to a 5.8 times lower risk of surgical complications and 11 times reduced risk of revision surgery. It is important to follow the progress of prospective randomized trials such as the MIS-ReFRESH study as more data are accumulated over longer time intervals. Staartjes et al[145] pooled 3 randomized controlled trials, and Lieber et al[28] are following 257 patients in a national inpatient sample with matched freehand controls. Gradually, implant accuracy should improve, complications should decrease, and revision rates should decrease as the early majority of fellowship-trained spinal surgeons gain more peer-reviewed and networked experience.

CONCLUSIONS

The fundamental technological challenge of navigation and robotic-assisted spinal surgery is that the virtual world needs to clearly represent the physical, real-time world. Navigational integrity and maintenance of fidelity in the transference of optoelectronic data is the cornerstone of robotic-assisted surgery. Transitioning from the controlled laboratory setting to the clinical operative environment requires an increased number of steps in the optoelectronic kinematic chain and potential for error propagation in experimental coordinate transformations. Moreover, intraoperative challenges of array location, system registration, spinal flexibility, anatomic topography, and workflow affect navigational integrity and provide a basis for the disparity of optoelectronic accuracy in the clinical environment compared with the controlled laboratory setting. A continuum of decreased accuracy is demonstrated when comparing the optoelectronic camera source itself with application in musculoskeletal platforms and, finally, the clinical operative environment. Diligence in the areas of preoperative planning, source camera and fiducial positioning, system registration, and intraoperative process workflow has the potential to improve accuracy and decrease disparity between planned and final implant position.

REFERENCES

1. van der Kruk E, Reijne MM. Accuracy of human motion capture systems for sport applications: state-of-the-art review. *Eur J Sport Sci*. 2018;18(6):806–819. doi:10.1080/17461391.2018.1463397

2. Linke D, Link D, Lames M. Validation of electronic performance and tracking systems EPTS under field conditions. *PLoS One*. 2018;13(7):e0199519. doi:10.1371/journal.pone.0199519

3. Linke D, Link D, Lames M. Football-specific validity of TRACAB's optical video tracking systems. *PLoS One*. 2020;15(3):e0230179. doi:10.1371/journal.pone.0230179

4. Elliott B, Alderson J. Laboratory versus field testing in cricket bowling: a review of current and past practice in modelling techniques. *Sports Biomech*. 2007;6(1):99–108. doi:10.1080/14763140601058623

5. Lindbeck L, Kjellberg K. Gender differences in lifting technique. *Ergonomics*. 2001;44(2):202–214. doi:10.1080/00140130120142

6. Nimbarte AD, Sun Y, Jaridi M, Hsiao H. Biomechanical loading of the shoulder complex and lumbosacral joints during dynamic cart pushing task. *Appl Ergon*. 2013;44(5):841–849. doi:10.1016/j.apergo.2013.02.008

7. Negrini S, Piovanelli B, Amici C, et al. Trunk motion analysis: a systematic review from a clinical and methodological perspective. *Eur J Phys Rehabil Med*. 2016;52(4):583–592.

8. Bravi M, Gallotta E, Morrone M, et al. Concurrent validity and inter trial reliability of a single inertial measurement unit for spatial-temporal gait parameter analysis in patients with recent total hip or total knee arthroplasty. *Gait Posture*. 2020;76:175–181. doi:10.1016/j.gaitpost.2019.12.014

9. Serrao M, Casali C, Ranavolo A, et al. Use of dynamic movement orthoses to improve gait stability and trunk control in ataxic patients. *Eur J Phys Rehabil Med*. 2017;53(5):735–743. doi:10.23736/S1973-9087.17.04480-X

10. Baker R. Gait analysis methods in rehabilitation. *J Neuroeng Rehabil*. 2006;3:4. doi:10.1186/1743-0003-3-4

11. Andújar D, Ribeiro Á, Fernández-Quintanilla C, Dorado J. Accuracy and feasibility of optoelectronic sensors for weed mapping in wide row crops. *Sensors (Basel)*. 2011;11(3):2304–2318. doi:10.3390/s110302304

12. Colyer SL, Evans M, Cosker DP, Salo AIT. A review of the evolution of vision-based motion analysis and the integration of advanced computer vision methods towards developing

a markerless system. *Sports Med Open*. 2018;4(1):24. doi:10.1186/s40798-018-0139-y

13. Cunningham BW, Sponseller PD, Murgatroyd AA, Kikkawa J, Tortolani PJ. A comprehensive biomechanical analysis of sacral alar iliac fixation: an in vitro human cadaveric model. *J Neurosurg Spine*. 2019;30(3):367–375. doi:10.3171/2018.8.SPINE18328

14. Cunningham BW, Mueller KB, Mullinix KP, Sun X, Sandhu FA. Biomechanical analysis of occipitocervical stabilization techniques: emphasis on integrity of osseous structures at the occipital implantation sites. *J Neurosurg Spine*. 2020;33(2):138–147. doi:10.3171/2020.1.spine191331

15. Dall BE, Eden SV, Cho W, et al. Biomechanical analysis of motion following sacroiliac joint fusion using lateral sacroiliac screws with or without lumbosacral instrumented fusion. *Clin Biomech (Bristol, Avon)*. 2019;68:182–189. doi:10.1016/j.clinbiomech.2019.05.025

16. Mushlin H, Brooks DM, Olexa J, et al. A biomechanical investigation of the sacroiliac joint in the setting of lumbosacral fusion: impact of pelvic fixation versus sacroiliac joint fixation. *J Neurosurg Spine*. 2019:1–6. doi:10.3171/2019.3.SPINE181127

17. Oxland TR. Fundamental biomechanics of the spine—what we have learned in the past 25 years and future directions. *J Biomech*. 2016;49(6):817–832. doi:10.1016/j.jbiomech.2015.10.035

18. La Barbera L, Wilke HJ, Liebsch C, et al. Biomechanical in vitro comparison between anterior column realignment and pedicle subtraction osteotomy for severe sagittal imbalance correction. *Eur Spine J*. 2020;29(1):36–44. doi:10.1007/s00586-019-06087-x

19. La Barbera L, Wilke HJ, Ruspi ML, et al. Load-sharing biomechanics of lumbar fixation and fusion with pedicle subtraction osteotomy. *Sci Rep*. 2021;11(1):3595. doi:10.1038/s41598-021-83251-8

20. Camino Willhuber G, Zderic I, Gras F, et al. Analysis of sacro-iliac joint screw fixation: does quality of reduction and screw orientation influence joint stability? A biomechanical study. *Int Orthop*. 2016;40(7):1537–1543. doi:10.1007/s00264-015-3007-0

21. Wang JQ, Wang Y, Feng Y, et al. Percutaneous sacroiliac screw placement: a prospective randomized comparison of robot-assisted navigation procedures with a conventional technique. *Chin Med J (Engl)*. 2017;130(21):2527–2534. doi:10.4103/0366-6999.217080

22. Wang M, Li D, Shang X, Wang J. A review of computer-assisted orthopaedic surgery systems. *Int J Med Robot*. 2020;16(5):1–28. doi:10.1002/rcs.2118

23. D'Souza M, Gendreau J, Feng A, Kim LH, Ho AL, Veeravagu A. robotic-assisted spine surgery: history, efficacy, cost, and future trends. *Robot Surg*. 2019;6:9–23. doi:10.2147/RSRR.S190720

24. Staub BN, Sadrameli SS. The use of robotics in minimally invasive spine surgery. *J Spine Surg*. 2019;5(suppl 1):S31–S40. doi:10.21037/jss.2019.04.16

25. Kim HJ, Jung WI, Chang BS, Lee CK, Kang KT, Yeom JS. A prospective, randomized, controlled trial of robot-assisted vs freehand pedicle screw fixation in spine surgery. *Int J Med Robot*. 2017;13(3). doi:10.1002/rcs.1779

26. Han X, Tian W, Liu Y, et al. Safety and accuracy of robot-assisted versus fluoroscopy-assisted pedicle screw insertion in thoracolumbar spinal surgery: a prospective randomized controlled trial. *J Neurosurg Spine*. 2019:1–8. doi:10.3171/2018.10.SPINE18487

27. Ahern DP, Gibbons D, Schroeder GD, Vaccaro AR, Butler JS. Image-guidance, robotics, and the future of spine surgery. *Clin Spine Surg*. 2020;33(5):179–184. doi:10.1097/BSD.0000000000000809

28. Lieber AM, Kirchner GJ, Kerbel YE, Khalsa AS. Robotic-assisted pedicle screw placement fails to reduce overall postoperative complications in fusion surgery. *Spine J*. 2019;19(2):212–217. doi:10.1016/j.spinee.2018.07.004

29. Sayari AJ, Pardo C, Basques BA, Colman MW. Review of robotic-assisted surgery: what the future looks like through a spine oncology lens. *Ann Transl Med*. 2019;7(10):224. doi:10.21037/atm.2019.04.69

30. Lieberman IH, Togawa D, Kayanja MM, et al. Bone-mounted miniature robotic guidance for pedicle screw and translaminar facet screw placement: Part I—technical development and a test case result. *Neurosurgery*. 2006;59(3):641–650; discussion 641–650. doi:10.1227/01.NEU.0000229055.00829.5B

31. Lieberman IH, Kisinde S, Hesselbacher S. Robotic-assisted pedicle screw placement during spine surgery. *JBJS Essent Surg Tech*. 2020;10(2):e0020. doi:10.2106/JBJS.ST.19.00020

32. Shoham M, Lieberman IH, Benzel EC, et al. Robotic assisted spinal surgery—from concept to clinical practice. *Comput Aided Surg*. 2007;12(2):105–115. doi:10.3109/10929080701243981

33. Ghasem A, Sharma A, Greif DN, Alam M, Maaieh MA. The arrival of robotics in spine surgery: a review of the literature. *Spine (Phila Pa 1976)*. 2018;43(23):1670–1677. doi:10.1097/BRS.0000000000002695

34. Helm PA, Teichman R, Hartmann SL, Simon D. Spinal navigation and imaging: history, trends, and future. *IEEE Trans Med Imaging*. 2015;34(8):1738–1746. doi:10.1109/TMI.2015.2391200

35. Zhang Q, Han XG, Xu YF, et al. Robotic navigation during spine surgery. *Expert Rev Med Devices*. 2020;17(1):27–32. doi:10.1080/17434440.2020.1699405

36. Devito DP, Kaplan L, Dietl R, et al. Clinical acceptance and accuracy assessment of spinal implants guided with SpineAssist surgical robot: retrospective study. *Spine (Phila Pa 1976)*. 2010;35(24):2109–2915. doi:10.1097/BRS.0b013e3181d323ab

37. Keric N, Doenitz C, Haj A, et al. Evaluation of robot-guided minimally invasive implantation of 2067 pedicle screws. *Neurosurg Focus*. 2017;42(5):E11. doi:10.3171/2017.2.FOCUS16552

38. Tarawneh AM, Salem KM. A systematic review and meta-analysis of randomized controlled trials comparing the accuracy and clinical outcome of pedicle screw placement using robot-assisted technology and conventional freehand technique. *Global Spine J*. 2021;11(4):575–586. doi:10.1177/2192568220927713

39. Cozzi Lepri A, Villano M, Innocenti M, Porciatti T, Matassi F, Civinini R. Precision and accuracy of robot-assisted technology with simplified express femoral workflow in measuring leg length and offset in total hip arthroplasty. *Int J Med Robot Comput Assist Surg*. 2020;16(5):1–6. doi:10.1002/rcs.2141

40. Xu S, Bernardo LIC, Yew AKS, Pang HN. Robotic-arm assisted direct anterior total hip arthroplasty: improving

implant accuracy. *Surg Technol Int*. 2020;38:sti38/1368. doi:10.52198/21.STI.38.OS1368

41. Deckey DG, Rosenow CS, Verhey JT, et al. Robotic-assisted total knee arthroplasty improves accuracy and precision compared to conventional techniques. *Bone Joint J*. 2021;103-B(6, suppl A):74–80. doi:10.1302/0301-620X.103B6.BJJ-2020-2003.R1

42. Jeon SW, Kim KI, Song SJ. Robot-assisted total knee arthroplasty does not improve long-term clinical and radiologic outcomes. *J Arthroplasty*. 2019;34(8):1656–1661. doi:10.1016/j.arth.2019.04.007

43. Goia A, Gilard V, Lefaucheur R, Welter ML, Maltête D, Derrey S. Accuracy of the robot-assisted procedure in deep brain stimulation. *Int J Med Robot*. 2019;15(6):e2032. doi:10.1002/rcs.2032

44. Grunert P, Darabi K, Espinosa J, Filippi R. Computer-aided navigation in neurosurgery. *Neurosurg Rev*. 2003;26(2):73–99; discussion 100–101. doi:10.1007/s10143-003-0262-0

45. Spörri J, Schiefermüller C, Müller E. Collecting kinematic data on a ski track with optoelectronic stereophotogrammetry: a methodological study assessing the feasibility of bringing the biomechanics lab to the field. *PLoS One*. 2016;11(8):e0161757. doi:10.1371/journal.pone.0161757

46. Richards JG. The measurement of human motion: a comparison of commercially available systems. *Hum Move Sci*. 1999;18(5):589–602. doi:10.1016/s0167-9457(99)00023-8

47. Topley M, Richards JG. A comparison of currently available optoelectronic motion capture systems. *J Biomech*. 2020;106:109820. doi:10.1016/j.jbiomech.2020.109820

48. Kantelhardt SR, Martinez R, Baerwinkel S, Burger R, Giese A, Rohde V. Perioperative course and accuracy of screw positioning in conventional, open robotic-guided and percutaneous robotic-guided, pedicle screw placement. *Eur Spine J*. 2011;20(6):860–868. doi:10.1007/s00586-011-1729-2

49. Lonjon N, Chan-Seng E, Costalat V, Bonnafoux B, Vassal M, Boetto J. Robot-assisted spine surgery: feasibility study through a prospective case-matched analysis. *Eur Spine J*. 2016;25(3):947–955. doi:10.1007/s00586-015-3758-8

50. Schatlo B, Molliqaj G, Cuvinciuc V, Kotowski M, Schaller K, Tessitore E. Safety and accuracy of robot-assisted versus fluoroscopy-guided pedicle screw insertion for degenerative diseases of the lumbar spine: a matched cohort comparison. *J Neurosurg Spine*. 2014;20(6):636–643. doi:10.3171/2014.3.SPINE13714

51. Schatlo B, Martinez R, Alaid A, et al. Unskilled unawareness and the learning curve in robotic spine surgery. *Acta Neurochir (Wien)*. 2015;157(10):1819–1823; discussion 1823. doi:10.1007/s00701-015-2535-0

52. Solomiichuk V, Fleischhammer J, Molliqaj G, et al. Robotic versus fluoroscopy-guided pedicle screw insertion for metastatic spinal disease: a matched-cohort comparison. *Neurosurg Focus*. 2017;42(5):E13. doi:10.3171/2017.3.FOCUS1710

53. Roser F, Tatagiba M, Maier G. Spinal robotics: current applications and future perspectives. *Neurosurgery*. 2013;72(suppl 1):A12–A18. doi:10.1227/NEU.0b013e318270d02c

54. Vadalà G, De Salvatore S, Ambrosio L, Russo F, Papalia R, Denaro V. Robotic spine surgery and augmented reality systems: a state of the art. *Neurospine*. 2020;17(1):88–100. doi:10.14245/ns.2040060.030

55. Zhang M, Wu B, Ye C, et al. Multiple instruments motion trajectory tracking in optical surgical navigation. *Opt Express*. 2019;27(11):15827–15845. doi:10.1364/OE.27.015827

56. Pechlivanis I, Kiriyanthan G, Engelhardt M, et al. Percutaneous placement of pedicle screws in the lumbar spine using a bone mounted miniature robotic system: first experiences and accuracy of screw placement. *Spine (Phila Pa 1976)*. 2009;34(4):392–398. doi:10.1097/BRS.0b013e318191ed32

57. Feng S, Tian W, Sun Y, Liu Y, Wei Y. Effect of robot-assisted surgery on lumbar pedicle screw internal fixation in patients with osteoporosis. *World Neurosurg*.2019;125:e1057–e1062. doi:10.1016/j.wneu.2019.01.243

58. Gertzbein SD, Robbins SE. Accuracy of pedicular screw placement in vivo. *Spine (Phila Pa 1976)*. 1990;15(1):11–14. doi:10.1097/00007632-199001000-00004

59. Euler angles. http://encyclopediaofmath.org/index.php?title=Euler_angles&oldid=34483. Accessed June 1, 2021.

60. Wu G, Siegler S, Allard P, et al. ISB recommendation on definitions of joint coordinate system of various joints for the reporting of human joint motion—part I: ankle, hip, and spine. *J Biomech*. 2002;35(4):543–548. doi:10.1016/s0021-9290(01)00222-6

61. Euler L. Formulae generales pro translatione quacunque corporum rigidorum. *Novi Commentari Acad Sci Imperalis Petropolitanae*. 1775;20:189–207,

62. Euler L. Nova methodus motum corporum rigidorum determinandi. *Novi Commentari Acad Sci Imperalis Petropolitanae*. 1775;20:208–238,

63. Saha SK. Denavit and Hartenberg (DH) parameters. In: *Introduction to Robotics*. 2nd ed. New York, NY: McGraw-Hill Education; 2014:15–18.

64. White AA, Panjabi MM. *Clinical Biomechanics of the Spine*. 2nd ed. Philadelphia, PA: Lippincott; 1990.

65. Panjabi MM. Biomechanical evaluation of spinal fixation devices: I. A conceptual framework. *Spine (Phila Pa 1976)*. 1988;13(10):1129–1134. doi:10.1097/00007632-198810000-00013

66. Panjabi MM, Abumi K, Duranceau J, Crisco JJ. Biomechanical evaluation of spinal fixation devices: II. Stability provided by eight internal fixation devices. *Spine (Phila Pa 1976)*. 1988;13(10):1135–1140. doi:10.1097/00007632-198810000-00014

67. International Organization for Standardization. ISO 5725-1 Accuracy (trueness and precision) of measurement methods and results. Part 1: General principles and definitions. 1994.

68. Elfring R, de la Fuente M, Radermacher K. Assessment of optical localizer accuracy for computer aided surgery systems. *Comput Aided Surg*. 2010;15(1–3):1–12. doi:10.3109/10929081003647239

69. Tamas Haidegger, Sándor Gyõri, Balazs Benyo, Zoltáán Benyó. Stochastic approach to error estimation for image-guided robotic systems *Annu Int Conf IEEE Eng Med Biol Soc*. 2010;2010:984–987 doi:10.1109/IEMBS.2010.5627624

70. Corazza S, Mündermann L, Gambaretto E, Ferrigno G, Andriacchi TP. Markerless motion capture through visual hull, articulated icp and subject specific model generation. *Int J Comput Vis*. 2010;87(1–2):156169. doi:10.1007/s11263-009-0284-3

71. Simon DA, Hebert M, Kanade T. Techniques for fast and accurate intrasurgical registration *J Image Guid Surg*. 1995;1(1):17–29. doi:10.1002/(SICI)1522-712X

72. Sielhorst T, Bauer M, Wenisch O, Klinker G, Navab N.

Online estimation of the target registration error for n-ocular optical tracking systems. *Med Image Comput Comput Assist Interv*. 2007;10(pt 2):652–659. doi:10.1007/978-3-540-75759-7_79

73. Koivukangas T, Katisko JP, Koivukangas JP. Technical accuracy of optical and the electromagnetic tracking systems. *Springerplus*. 2013;2(1):90. doi:10.1186/2193-1801-2-90

74. Maletsky LP, Sun J, Morton NA. Accuracy of an optical active-marker system to track the relative motion of rigid bodies. *J Biomech*. 2007;40(3):682–685. doi:10.1016/j.jbiomech.2006.01.017

75. Chassat F, Lavallée S. Experimental protocol of accuracy evaluation of 6-d localizers for computer-integrated surgery: application to four optical localizers. *Medical Image Computing and Computer-Assisted Intervention—MICCAI'98*. 1998:277–284. doi:10.1007/bfb0056211

76. Citak M, Kendoff D, Wanich T, et al. The influence of distance on registration in ISO-C-3D navigation: a source of error in ISO-C-3D navigation. *Technol Health Care*. 2006;14(6):473–478.

77. Fitzpatrick JM, West JB, Maurer CR. Predicting error in rigid-body point-based registration. *IEEE Trans Med Imaging*. 1998;17(5):694–702. doi:10.1109/42.736021

78. Wiles AD, Thompson DG, Frantz DD. Accuracy assessment and interpretation for optical tracking systems. In Galloway Jr R,ed.Proceedings Medical Imaging 2004: Visualization, Image-Guided Procedures, and Display. 2004;5367. doi:10.1117/12.536128

79. Fitzpatrick JM, West JB. The distribution of target registration error in rigid-body point-based registration. *IEEE Trans Med Imaging*. 2001;20(9):917–927. doi:10.1109/42.952729

80. Windolf M, Götzen N, Morlock M. Systematic accuracy and precision analysis of video motion capturing systems—exemplified on the Vicon-460 system. *J Biomech*. 2008;41(12):2776–2780. doi:10.1016/j.jbiomech.2008.06.024

81. Stancic I, Grujic Supuk T, Panjkota A. Design, development and evaluation of optical motion-tracking system based on active white light markers. *IET Sci Meas Technol*. 2013;7(4):206–214. doi:10.1049/iet-smt.2012.0157

82. Khadem R, Yeh CC, Sadeghi-Tehrani M, et al. Comparative tracking error analysis of five different optical tracking systems. *Comput Aided Surg*. 2000;5(2):98–107. doi:10.1002/1097-0150(2000)5:2<98::AID-IGS4>3.0.CO;2-H

83. Wilke H, Fischer K, Jeanneret B, Claes L, Magerl F. In-vivo-Messung der dreidimensionalen Bewegung des Iliosakralgelenks. *Z Orthop Ihre Grenzgebiet*. 2008;135:550–556.

84. Bowden AE, Guerin HL, Villarraga ML, Patwardhan AG, Ochoa JA. Quality of motion considerations in numerical analysis of motion restoring implants of the spine. *Clin Biomech (Bristol, Avon)*. 2008;23(5):536–544. doi:10.1016/j.clinbiomech.2007.12.010

85. Ilharreborde B, Zhao K, Boumediene E, Gay R, Berglund L, An KN. A dynamic method for in vitro multisegment spine testing. *Orthop Traumatol Surg Res*. 2010;96(4):456–461. doi:10.1016/j.otsr.2010.01.006

86. Jeong JH, Leasure JM, Park J. Assessment of biomechanical changes after sacroiliac joint fusion by application of the 3-dimensional motion analysis technique. *World Neurosurg*. 2018;117:e538–e543. doi:10.1016/j.wneu.2018.06.072

87. Osterhoff G, Dodd AE, Unno F, et al. Cement augmentation in sacroiliac screw fixation offers modest biomechanical advantages in a cadaver model. *Clin Orthop Relat Res*. 2016;474(11):2522–2530. doi:10.1007/s11999-016-4934-9

88. Osterhoff G, Tiziani S, Hafner C, Ferguson SJ, Simmen HP, Werner CM. Symphyseal internal rod fixation versus standard plate fixation for open book pelvic ring injuries: a biomechanical study. *Eur J Trauma Emerg Surg*. 2016;42(2):197–202. doi:10.1007/s00068-015-0529-5

89. Hammer N, Scholze M, Kibsgård T, et al. Physiological in vitro sacroiliac joint motion: a study on three-dimensional posterior pelvic ring kinematics. *J Anat*. 2019;234(3):346–358. doi:10.1111/joa.12924

90. Baria D, Lindsey RW, Milne EL, Kaimrajh DN, Latta LL. Effects of lumbosacral arthrodesis on the biomechanics of the sacroiliac joint. *JB JS Open Access*. 2020;5(1):e0034. doi:10.2106/JBJS.OA.19.00034

91. Sun M, Chai Y, Chai G, Zheng X. Fully automatic robot-assisted surgery for mandibular angle split osteotomy. *J Craniofac Surg*. 2020 2020;31(2):336–339. doi:10.1097/SCS.0000000000005587

92. Guo N, Wang T, Wei M, et al. An ACL reconstruction robotic positioning system based on anatomical characteristics. *Int J Adv Robot Syst*. 2020;17(1):172988141988616. doi:10.1177/1729881419886160

93. Hampp EL, Chughtai M, Scholl LY, et al. Robotic-arm assisted total knee arthroplasty demonstrated greater accuracy and precision to plan compared with manual techniques. *J Knee Surg*. 2019;32(3):239–250. doi:10.1055/s-0038-1641729

94. Miller JG, Li M, Mazilu D, Hunt T, Horvath KA. Robot-assisted real-time magnetic resonance image-guided transcatheter aortic valve replacement. *J Thorac Cardiovasc Surg*. 2016;151(5):1407–1412. doi:10.1016/j.jtcvs.2015.11.047

95. Liu WP, Richmon JD, Sorger JM, Azizian M, Taylor RH. Augmented reality and cone beam CT guidance for transoral robotic surgery. *J Robot Surg*. 2015;9(3):223–233. doi:10.1007/s11701-015-0520-5

96. Kalia M, Mathur P, Tsang K, Black P, Navab N, Salcudean S. Evaluation of a marker-less, intra-operative, augmented reality guidance system for robot-assisted laparoscopic radical prostatectomy. *Int J Comput Assist Radiol Surg*. 2020;15(7):1225–1233. doi:10.1007/s11548-020-02181-4

97. Diakov G, Freysinger W. Vector field analysis for surface registration in computer-assisted ENT surgery. *Int J Med Robot*. 2019;15(2):e1977. doi:10.1002/rcs.1977

98. Kwartowitz DM, Herrell SD, Galloway RL. Toward image-guided robotic surgery: determining intrinsic accuracy of the da Vinci robot. *Int J Comput Assist Radiol Surg*. 2006;1(3):157–165. doi:10.1007/s11548-006-0047-3

99. Kwartowitz DM, Herrell SD, Galloway RL. Update: Toward image-guided robotic surgery: determining the intrinsic accuracy of the da Vinci-S robot. *Int J Comput Assist Radiol Surg*. 2007;1(5):301–304. doi:10.1007/s11548-006-0064-2

100. Ringel F, Stüer C, Reinke A, et al. Accuracy of robot-assisted placement of lumbar and sacral pedicle screws: a prospective randomized comparison to conventional freehand screw implantation. *Spine (Phila Pa 1976)*. 2012;37(8):E496–E501. doi:10.1097/BRS.0b013e31824b7767

101. Fan Y, Du JP, Liu JJ, et al. Accuracy of pedicle screw placement comparing robot-assisted technology and the free-hand with fluoroscopy-guided method in spine surgery: an updated meta-analysis. *Medicine (Baltimore)*. 2018;97(22):e10970. doi:10.1097/md.0000000000010970

102. Fan M, Liu Y, He D, et al. Improved accuracy of cervical spinal surgery with robot-assisted screw insertion: a prospective, randomized, controlled study. *Spine (Phila Pa 1976)*. 2020;45(5):285–291. doi:10.1097/BRS.0000000000003258

103. Huang M, Tetreault TA, Vaishnav A, York PJ, Staub BN. The current state of navigation in robotic spine surgery. *Ann Transl Med*. 2021;9(1):86. doi:10.21037/atm-2020-ioi-07

104. Kalidindi KKV, Sharma JK, Jagadeesh NH, Sath S, Chhabra HS. Robotic spine surgery: a review of the present status. *J Med Eng Technol*. 2020;44(7):431–437. doi:10.1080/03091902.2020.1799098

105. Elswick CM, Strong MJ, Joseph JR, Saadeh Y, Oppenlander M, Park P. Robotic-assisted spinal surgery: current generation instrumentation and new applications. *Neurosurg Clin N Am*. 2020;31(1):103–110. doi:10.1016/j.nec.2019.08.012

106. Overley SC, Cho SK, Mehta AI, Arnold PM. Navigation and robotics in spinal surgery: where are we now? *Neurosurgery*. 2017;80(3S):S86–S99. doi:10.1093/neuros/nyw077

107. Yu X, Xu L, Bi LY. [Spinal navigation with intra-operative 3D-imaging modality in lumbar pedicle screw fixation]. *Zhonghua Yi Xue Za Zhi*. 2008;88(27):1905–1908.

108. Yu CC, Bajwa NS, Toy JO, Ahn UM, Ahn NU. Pedicle morphometry of upper thoracic vertebrae: an anatomic study of 503 cadaveric specimens. *Spine (Phila Pa 1976)*. 2014;39(20):E1201–E1209. doi:10.1097/BRS.0000000000000505

109. Yu L, Chen X, Margalit A, Peng H, Qiu G, Qian W. Robot-assisted vs freehand pedicle screw fixation in spine surgery—a systematic review and a meta-analysis of comparative studies. *Int J Med Robot*. 2018;14(3):e1892. doi:10.1002/rcs.1892

110. Vardiman AB, Wallace DJ, Booher GA, et al. Does the accuracy of pedicle screw placement differ between the attending surgeon and resident in navigated robotic-assisted minimally invasive spine surgery? *J Robot Surg*. 2020;14(4):567–572. doi:10.1007/s11701-019-01019-9

111. Vardiman AB, Wallace DJ, Crawford NR, Riggleman JR, Ahrendtsen LA, Ledonio CG. Pedicle screw accuracy in clinical utilization of minimally invasive navigated robot-assisted spine surgery. *J Robot Surg*. 2020;14(3):409–413. doi:10.1007/s11701-019-00994-3

112. Chen HY, Xiao XY, Chen CW, et al. Results of using robotic-assisted navigational system in pedicle screw placement. *PLoS One*. 2019;14(8):e0220851. doi:10.1371/journal.pone.0220851

113. Chen HY, Xiao XY, Chen CW, et al. A spine robotic-assisted navigation system for pedicle screw placement. *J Vis Exp*. 2020;(159). doi:10.3791/60924

114. Chen L, Zhang F, Zhan W, Gan M, Sun L. Research on the accuracy of three-dimensional localization and navigation in robot-assisted spine surgery. *Int J Med Robot*. 2020;16(2):e2071. doi:10.1002/rcs.2071

115. Togawa D, Kayanja MM, Reinhardt MK, et al. Bone-mounted miniature robotic guidance for pedicle screw and translaminar facet screw placement: part 2–Evaluation of system accuracy. *Neurosurgery*. 2007;60(2, suppl 1):ONS129–ONS139; discussion ONS139. doi:10.1227/01.NEU.0000249257.16912.AA

116. Macke JJ, Woo R, Varich L. Accuracy of robot-assisted pedicle screw placement for adolescent idiopathic scoliosis in the pediatric population. *J Robot Surg*. 2016;10(2):145–150. doi:10.1007/s11701-016-0587-7

117. Fu W, Tong J, Liu G, et al. Robot-assisted technique vs conventional freehand technique in spine surgery: a meta-analysis. *Int J Clin Pract*. 2020:e13964. doi:10.1111/ijcp.13964

118. Huntsman KT, Riggleman JR, Ahrendtsen LA, Ledonio CG. Navigated robot-guided pedicle screws placed successfully in single-position lateral lumbar interbody fusion. *J Robot Surg*. 2020;14(4):643–647. doi:10.1007/s11701-019-01034-w

119. Johnson N. Imaging, navigation, and robotics in spine surgery. *Spine (Phila Pa 1976)*. 2016;41(suppl 7):S32. doi:10.1097/BRS.0000000000001437

120. Kochanski RB, Lombardi JM, Laratta JL, Lehman RA, O'Toole JE. Image-guided navigation and robotics in spine surgery. *Neurosurgery*.2019;84(6):1179–1189. doi:10.1093/neuros/nyy630

121. Kotani Y, Abumi K, Ito M, Minami A. Improved accuracy of computer-assisted cervical pedicle screw insertion. *J Neurosurg*. 2003;99(suppl 3):257–263. doi:10.3171/spi.2003.99.3.0257

122. Le X, Tian W, Shi Z, et al. Robot-assisted versus fluoroscopy-assisted cortical bone trajectory screw instrumentation in lumbar spinal surgery: a matched-cohort comparison. *World Neurosurg*. 2018;120:e745–e751. doi:10.1016/j.wneu.2018.08.157

123. Sukovich W, Brink-Danan S, Hardenbrook M. Miniature robotic guidance for pedicle screw placement in posterior spinal fusion: early clinical experience with the SpineAssist. *Int J Med Robot*. 2006;2(2):114–22. doi:10.1002/rcs.86

124. Vo CD, Jiang B, Azad TD, Crawford NR, Bydon A, Theodore N. Robotic spine surgery: current state in minimally invasive surgery. *Global Spine J*. 2020;10(suppl 2):34S–40S. doi:10.1177/2192568219878131

125. Wallace DJ, Vardiman AB, Booher GA, et al. Navigated robotic assistance improves pedicle screw accuracy in minimally invasive surgery of the lumbosacral spine: 600 pedicle screws in a single institution. *Int J Med Robot*. 2020;16(1):e2054. doi:10.1002/rcs.2054

126. West JB, Fitzpatrick JM, Toms SA, Maurer CR, Maciunas RJ. Fiducial point placement and the accuracy of point-based, rigid body registration. *Neurosurgery*. 2001;48(4):810–816; discussion 816–817. doi:10.1097/00006123-200104000-00023

127. West JB, Maurer CR. Designing optically tracked instruments for image-guided surgery. *IEEE Trans Med Imaging*. 2004;23(5):533–545. doi:10.1109/tmi.2004.825614

128. Jiang B, Pennington Z, Zhu A, et al. Three-dimensional assessment of robot-assisted pedicle screw placement accuracy and instrumentation reliability based on a preplanned trajectory. *J Neurosurg Spine*. 2020:1–10. doi:10.3171/2020.3.SPINE20208

129. Weinstein JN, Spratt KF, Spengler D, Brick C, Reid S. Spinal pedicle fixation: reliability and validity of roentgenogram-based assessment and surgical factors on successful screw placement. *Spine (Phila Pa 1976)*. 1988;13(9):1012–1018. doi:10.1097/00007632-198809000-00008

130. Shuford MD. Robotically assisted laparoscopic radical prostatectomy: a brief review of outcomes. *Baylor Univ Med Center Proc*. 2007;20(4):354–356. doi:10.1080/08998280.2007.11928322

131. Koh DH, Jang WS, Park JW, et al. Efficacy and safety of robotic procedures performed using the da Vinci robotic surgical system at a single institute in Korea: experience with 10000 cases. *Yonsei Med J*. 2018;59(8):975. doi:10.3349/ymj.2018.59.8.975

132. Murphy DG, Hall R, Tong R, Goel R, Costello AJ. Robotic technology in surgery: current status in 2008. *ANZ J Surg*. 2008;78(12):1076–1081. doi:10.1111/j.1445-2197.2008.04754.x

133. Cunningham BW, Brooks DM. Comparative analysis of optoelectronic accuracy in the laboratory setting versus clinical operative environment—a systematic review. *Global Spine J – Focus Edition Navigation and Robotics*. 2021.

134. Avrunin OG, Alkhorayef M, Farouk Ismail Saied H, Tymkovych MY. The surgical navigation system with optical position determination technology and sources of errors. *J Med Imaging Health Inform*. 2015;5. doi:10.1166/jmihi.2015.1444

135. Garg B, Mehta N, Malhotra R. Robotic spine surgery: ushering in a new era. *J Clin Orthop Trauma*. 2020;11(5):753–760. doi:10.1016/j.jcot.2020.04.034

136. Hu X, Ohnmeiss DD, Lieberman IH. Robotic-assisted pedicle screw placement: lessons learned from the first 102 patients. *Eur Spine J*. 2013;22(3):661–666. doi:10.1007/s00586-012-2499-1

137. Hu X, Lieberman IH. What is the learning curve for robotic-assisted pedicle screw placement in spine surgery? *Clin Orthop Relat Res*. 2014;472(6):1839–1844. doi:10.1007/s11999-013-3291-1

138. Min Z, Zhu D, Meng MQ-H. Accuracy assessment of an N-ocular motion capture system for surgical tool tip tracking using pivot calibration. IEEE Conference; August 2016. doi:10.1109//ICInfA.2016.7832079

139. Abbasi HR, Grzeszczuk R, Chin S, et al. Clinical fluoroscopic fiducial-based registration of the vertebral body in spinal neuronavigation. *Stud Health Technol Inform*. 2001;81:1–7.

140. Hüfner T, Geerling J, Oldag G, et al. Accuracy study of computer-assisted drilling: the effect of bone density, drill bit characteristics, and use of a mechanical guide. *J Orthop Trauma*. 2005;19(5):317–322.

141. Messmer P, Gross T, Suhm N, Regazzoni P, Jacob AL, Huegli RW. Modality-based navigation. *Injury*. 2004;35(suppl 1):S-A24–S-A29. doi:10.1016/j.injury.2004.05.007

142. Rahmathulla G, Nottmeier EW, Pirris SM, Deen HG, Pichelmann MA. Intraoperative image-guided spinal navigation: technical pitfalls and their avoidance. *Neurosurgical Focus*. 2014;36(3):E3. doi:10.3171/2014.1.focus13516

143. Crawford N, Johnson N, Theodore N. Ensuring navigation integrity using robotics in spine surgery. *J Robot Surg*. 2020;14(1):177–183. doi:10.1007/s11701-019-00963-w

144. Good CR, Orosz L, Schroerlucke SR, et al. Complications and revision rates in minimally invasive robotic-guided versus fluoroscopic-guided spinal fusions: the MIS ReFRESH Prospective Comparative Study. *Spine (Phila Pa 1976)*. 2021. doi:10.1097/BRS.0000000000004048

145. Staartjes VE, Klukowska AM, Schröder ML. pedicle screw revision in robot-guided, navigated, and freehand thoracolumbar instrumentation: a systematic review and meta-analysis. *World Neurosurg*. 2018;116:433–443.e8. doi:10.1016/j.wneu.2018.05.159

Corresponding Author: Bryan W. Cunningham, PhD, Department of Orthopaedic Surgery, MedStar Union Memorial Hospital, 201 East University Parkway, Baltimore, MD 21218. Phone: (410) 554-4368; Email: bcspine@gmail.com.

Published 0 Month 2021